Available online at www.sciencedirect.com
ScienceDirect
Journal of Molecular Catalysis A: Chemical 281 (2008) 3–8
JOURNAL OF MOLECULAR CATALYSIS A: CHEMICAL
www.elsevier.com/locate/molcata

Crystallographic structure of ultra-thin films of Pd on Ni(1 1 1) and Ni on Pd(1 1 1) studied by photoelectron diffraction

P.A.P. Nascente [a,*], M.F. Carazzolle [b], A. de Siervo [b,c], S.S. Maluf [a], R. Landers [b,c], G.G. Kleiman [b]

[a] *Universidade Federal de São Carlos, Departamento de Engenharia de Materiais, 13565-905 São Carlos, SP, Brazil*
[b] *Universidade Estadual de Campinas, Instituto de Física "Gleb Wataghin", Departamento de Física Aplicada, 13083-970 Campinas, SP, Brazil*
[c] *Laboratório Nacional da Luz Síncrotron, 13083-970 Campinas, SP, Brazil*

Available online 29 September 2007

Abstract

We report studies of ultra-thin films of Pd and Ni deposited on Ni(1 1 1) and Pd(1 1 1) surfaces, respectively, using X-ray photoelectron spectroscopy (XPS), low-energy electron diffraction (LEED), and X-ray photoelectron diffraction (XPD). For a 1.5 ML Pd film deposited on Ni(1 1 1) at room temperature, XPS indicates that Pd grows in a layer-by-layer fashion and does not diffuse on the Ni substrate, whereas LEED exhibits a reconstructed pattern, which can be attributed to a distribution of bi-dimensional islands on the surface with a lateral lattice parameter different from that of Ni(1 1 1). Annealing the film at 650 °C produces a (1 × 1) LEED pattern, which suggests Pd diffusion and alloy formation. By using a systematic XPD analysis, we were able to determine that Pd diffused at least to the fourth layer into the Ni(1 1 1) substrate in low concentrations (10–20%), and that 75% of the surface remained covered by Pd bi-dimensional islands. The complementary system, Ni on Pd(1 1 1), presented similar LEED and XPS results. The comparison between experimental and theoretical XPD results indicated that the surface was partially covered by Ni islands (50–60%), and the other part was formed by random Ni_xPd_{100-x} surface alloy.

Keywords: X-ray photoelectron diffraction; Synchrotron radiation; Low-energy electron diffraction; Surface alloys; Nickel films; Palladium films

1. Introduction

Bimetallic surfaces have been investigated due to their interesting catalytic, electronic, electrochemical, and magnetic properties [1,2]. The deposition of an ultra-thin metal film on a single crystal metal substrate can produce a bimetallic surface. The films constituted by transition and noble metals present particular interest in heterogeneous catalysis, since bimetallic surfaces have shown an enhanced activity for catalytic reaction as compared to pure metals [2]. The interfacial interactions between the two metals can lead to preferential surface orientations, surface relaxation, surface reconstruction, order/disordered effects, and surface alloying [1,3]. Ni-Pd presents a complete solid solution in the bulk, but significant Pd surface enrichment was found in polycrystalline bulk alloys [4], alloy films [5], and single crystal alloys [6–9].

Hermann et al. [10] studied ultra-thin films of palladium deposited on Ni(1 1 1) surface as a model catalyst for the hydrogenation of 1,3-butadiene. They found that Pd stays on the surface up to 400 °C and diffuses into the bulk for higher temperatures [10]. Terada et al. [11] used scanning tunneling microscopy (STM) to investigate the growth mechanism of Pd layers on Ni(1 1 1) deposited at room temperature. They reported a two-dimensional Pd growth up to the third layer [11]. Rizzi et al. [12,13] studied by means of LEED and XPD the epitaxial growth of ultra-thin Ni films deposited on Pd(1 0 0). They identified a tetragonally strained face centered Ni phase in the early stages of the deposition, and a bulk-like fcc structure above 9–12 layers [12,13]. Manzhur et al. [14] reported on the magnetic properties of strained ultra-thin Ni films on Pd(1 0 0) and concluded that the magnetic anisotropy of 2 ML of Ni(1 0 0) is different than the Ni(1 0 0) surface of a bulk crystal.

This work is an extension of our previous studies on the Ni-Pd system [15,16]. In this paper, we report our studies of the growth, composition, and structure of ultra-thin films of Pd and Ni deposited on Ni(1 1 1) and Pd(1 1 1), respectively. We charac-

* Corresponding author. Tel.: +55 16 33518828; fax: +55 16 33615404.
E-mail address: nascente@ufscar.br (P.A.P. Nascente).

1381-1169/$ – see front matter © 2007 Elsevier B.V. All rights reserved.
doi:10.1016/j.molcata.2007.09.021

terized the ultra-thin films by means of XPS, LEED, and XPD. For the Pd on Ni(1 1 1) system, we demonstrate the quality of the agreement between our final model of a surface partially covered (∼50%) by islands and partially by an alloy and the XPD data. For the system of Ni on Pd(1 1 1) we demonstrate in detail the various steps in determining the final structure of partial island coverage. Preliminary results for this system were reported already [16].

2. Experimental and theoretical methods

The 10 mm diameter Ni(1 1 1) and Pd(1 1 1) crystals were mounted on thick Ta foil supports that could be aligned by laser with three set screws. The experiments were performed at the Brazilian Synchrotron Radiation Laboratory (LNLS) using the bending magnet beam line with a Spherical Grating Monochromator (SGM), and the measurements were done with a surface analysis system equipped with LEED optics, a high resolution electron analyzer (Omicron HA125HR with multi-detection) mounted in the plane of the storage ring, a differentially pumped argon ion sputter gun, a two axis sample manipulator [17] and a conventional Al Kα (1486.6 eV) X-ray source. The base pressure was always less than 2×10^{-10} Torr during the analyses.

The Ni(1 1 1) and Pd(1 1 1) crystals were cleaned in UHV by cycles of argon ion sputtering (1.0 μA mm^{-2} current density and 1 kV accelerating potential) and annealed using an electron beam (20 mA, 1.0 kV) impinging on the backside of the crystal to heat the sample. We considered the surfaces to be clean when typical contaminants such as C, O, N and S were not detected by XPS, and the LEED displayed well-defined (1 × 1) patterns.

Pd and Ni wire tips heated by electron bombardment were the source for depositing the Pd and Ni films onto the Ni(1 1 1) and Pd(1 1 1) substrates at room temperature with subsequent annealing at different temperatures. We calibrated the evaporation flux by using the Pd and Ni XPS signals according to two different methods: that is, by following the growth process in real-time with XPS and by using an angle resolved XPS analysis. The fluxes were approximately 1 and 0.3 ML min^{-1} for the Pd and Ni films, respectively.

We performed the angular XPD measurements by varying the azimuthal angle, in steps of 3° over a range of 129°, which guaranteed measurement of all the diffraction features, and generated the complete 360° azimuth curve by exploiting the three-fold symmetry. The polar angle, defined as the angle between the analyzer axis and the surface normal, varied from 20° to 60° in steps of 5°. We used two photon energies: 700 eV and 1486.6 eV, which yield, respectively, approximately the same kinetic energy (i.e., ∼633 eV) and scattering regime (i.e., forward scattering) for the Ni 3p and 2p photoelectrons. The Pd 3d photoelectron for the lower photon energy has a kinetic energy of around 360 eV, corresponding to a mean free path of around 7.6 Å and a scattering regime with a sizeable backscattering contribution; the Pd 3d photoelectron for the higher energy has a kinetic energy of around 1150 eV, corresponding to a mean free path of around 15 Å and a forward scattering regime. The photoelectron diffraction patterns measured with these kinetic energies have considerable multiple scattering contributions and their simulation was possible only through a comprehensive multiple scattering theory approach.

In order to simulate the XPD patterns, we employed the MSCD code [18], including an ATA-Average T-matrix approximation subroutine that makes the program able to simulate ordered and random alloy systems [19]. The phase shifts were obtained using the muffin tin potential for Ni and Pd in their bulk phases. The model clusters had paraboloid shapes with 12 Å radius and 18 Å depth, corresponding approximately to 290 atoms. This cluster configuration allowed us to avoid the most significant boundary effects in the multiple scattering calculations and to perform simulations for the high kinetic energy Pd 3d photoelectrons.

XPD analysis of surfaces partially covered with islands of adsorbates is a complicated problem. We treat this problem in the following way: first, we determine the island structural parameters by simulating the spectra sensitive to the island structure; we then treat the possibility of alloy formation on the rest of the surface by simulating the spectra insensitive to the island structure; finally, we use a linear combination of the theoretical intensities from the portion of the surface covered by islands and from the portion free of islands (with the structural and alloy concentration parameters determined previously), and assume that the weights in the linear combination (found by fitting the experimental XPD data) are proportional to the areas covered by the islands and those free of the islands. The reliability of the theoretical simulations as compared to the experimental data was measured through the well-established *R*-factor analysis [18].

3. Results and discussion

3.1. Pd on Ni(1 1 1) at room temperature

Ultra-thin films of palladium grew bi-dimensionally on the Ni(1 1 1) surface at room temperature, as determined by the ratio of the Pd 3d and Ni 3p XPS peaks [15]. This layer-by-layer growth was reported in the literature [10,11]. We used angle-resolved XPS to determine the film thickness, and, for an equivalent 1.5 ML evaporated and as-grown Pd film, the model which best fit the data corresponded to a combination of one complete overlayer (100% of Pd in 1 ML) followed by a second incomplete layer [15].

The LEED pattern for 1.5 ML of Pd evaporated on Ni(1 1 1) at room temperature showed double spots around the (1 × 1) pattern [15], resembling a Moiré coincidence pattern, which can be associated with the formation of Pd islands [11]. We attributed the double radial spots to the difference between the lattice parameters of the Ni substrate and the Pd islands. A simple geometrical analysis of the LEED pattern indicated that the lateral lattice parameter of the Pd islands was approximately 2.61 ± 0.05 Å (approximately 3.8% greater that that of the clean Ni(1 1 1) surface) [15]. Annealing at 500 °C did not change much the LEED pattern, except for a small decrease in the diffuse background. Annealing at 650 °C caused a coalescence of the double spots, producing rather large single spots in a pattern similar to that of Ni(1 1 1) [15].

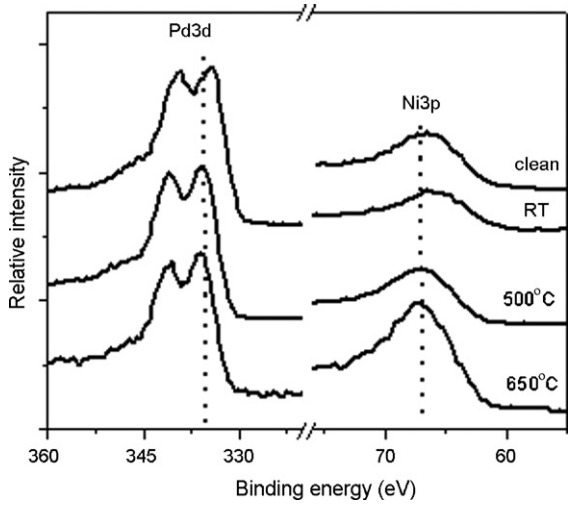

Fig. 1. Ni 3p and Pd 3d XP-spectra: clean Ni surface, 1.5 ML Pd film at room temperature, after annealing at 500 °C, and after annealing at 650 °C.

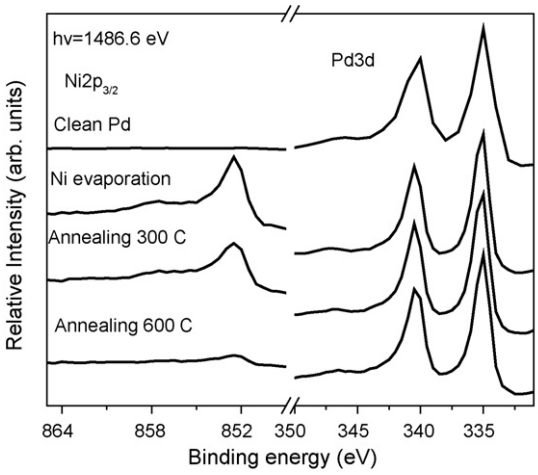

Fig. 3. Ni 3p and Pd 3d XP-spectra for Ni on Pd(1 1 1). From top to bottom we present, respectively, results for: the clean Pd surface, the Ni film evaporated at room temperature, the film annealed at 300 °C, and the film annealed at 600 °C.

Fig. 1 displays the Ni 3p and Pd 3d photoemission spectra obtained for the clean Ni surface (the top spectrum), the 1.5 ML Pd film at room temperature (the second highest spectrum), after annealing at 500 °C (next to lowest spectrum), and after annealing at 650 °C (lowest spectrum). We observe a systematic enhancement of the Ni 3p signal with the annealing temperature, especially for 650 °C. However, basing only on this XPS data it is very difficult to assess whether the Pd is diffusing into the bulk and Ni is segregating to the surface, or whether Pd is coalescing into islands, leaving areas of clean Ni surface.

3.2. Pd on Ni(1 1 1) after annealing at 650 °C

To determine the surface structure we considered models consisting of (1) Pd overlayers with 0–4 ML height completely covering the Ni(1 1 1) surface and occupying either hcp or fcc sites, (2) random alloy of different concentrations in the first four atomic layers, and (3) coexistence of regions on the surface with 1–4 ML islands and regions of a Pd_xNi_{100-x} alloy, which is a combination of the first two models. For each model, the interlayer and intra-layer distances were relaxed.

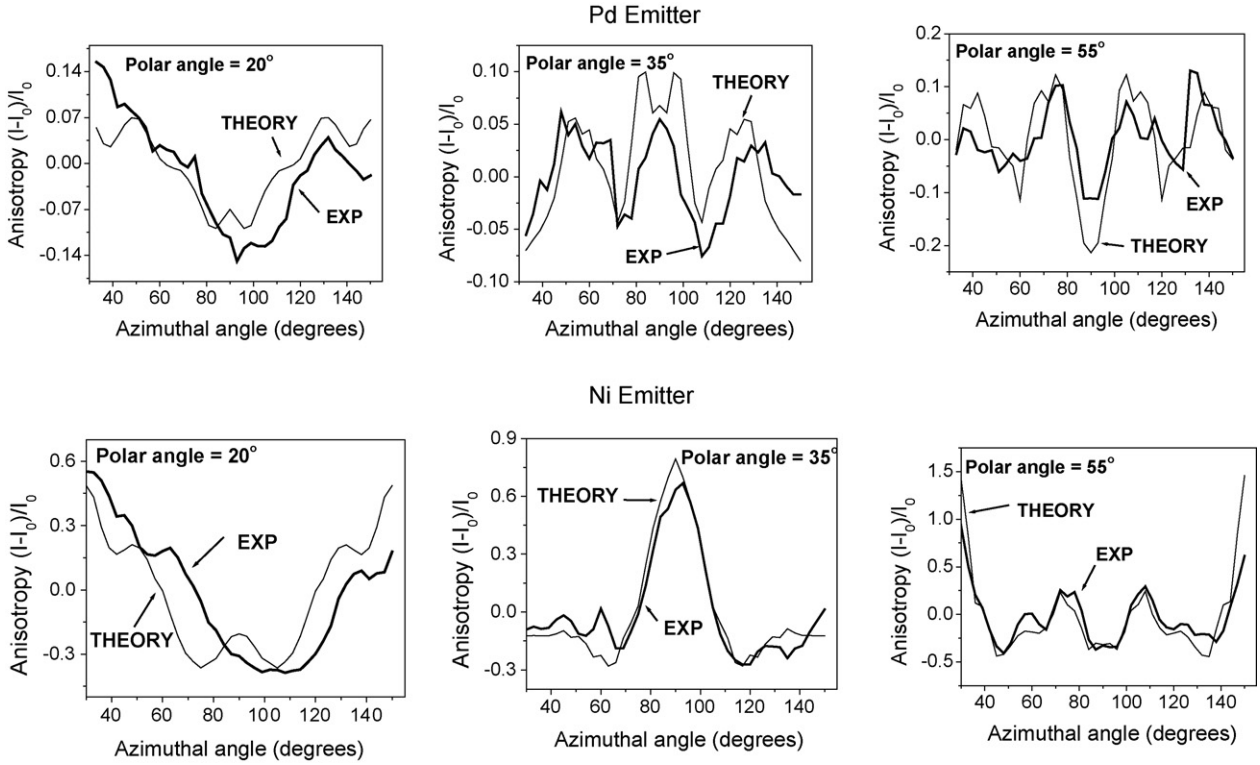

Fig. 2. Illustration, for Pd on Ni(1 1 1), of the agreement between theoretical and experimental XPD intensities as a function of the azimuthal angle. The top row correspond to the Pd 3d emitter and the bottom to the Ni 3p emitter. The photon energy was 700 eV.

For the Ni emitter, the best results for the reliability factor R_a (defined in Refs. [17] and [19]), in the *R*-factor analysis for each case are 0.19, 0.35, 0.48, 0.49, and 0.52, respectively, for the clean Ni surface, and the 1–4 ML height Pd islands [15]. The best model was the one associated to the clean Ni(1 1 1) surface, indicating that the Ni 3p XPD is relatively insensitive to the presence of Pd islands**,** and that the Ni substrate has bare regions [15]. For the Pd emitter, the R_a-factor analysis yielded unacceptable results for both the first and second models: the R_a-factor for the first model, with a 1 ML height overlayer of Pd occupying FCC sites, was approximately 0.6, for the first model, and that for the second model was higher than 0.6. When we

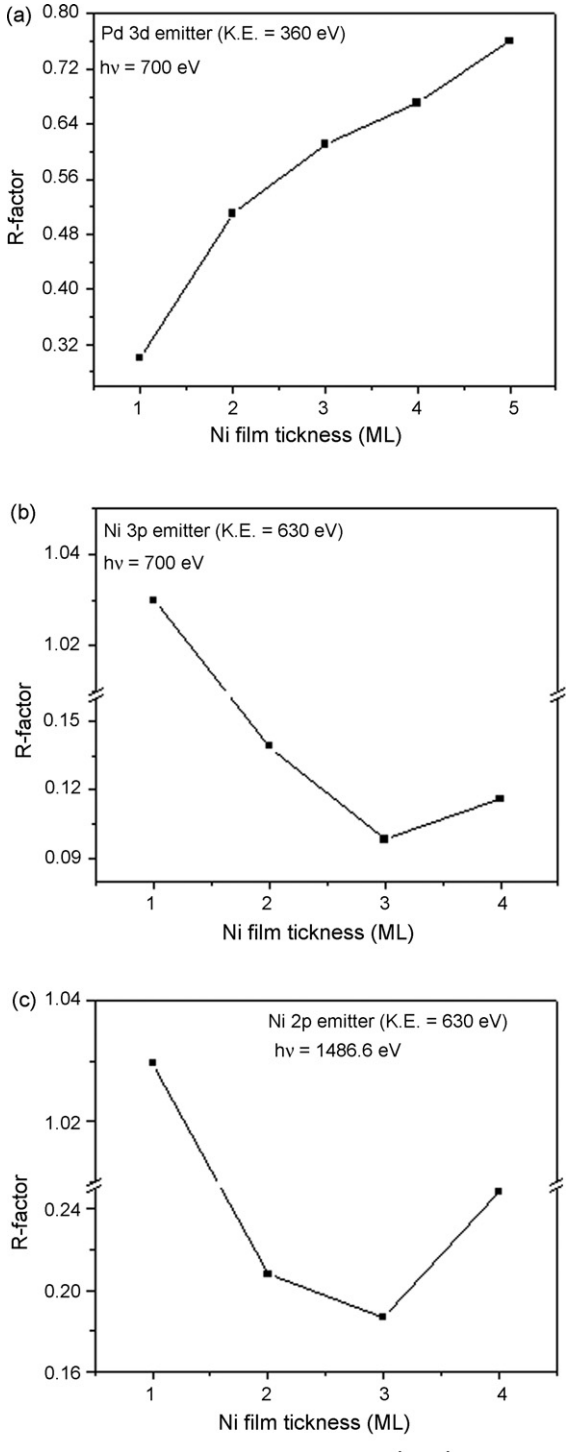

Fig. 4. *R*-factor analysis for the Pd 3d and Ni 3p emitters, with $h\nu = 700$ eV, and for the Ni 2p emitter, with $h\nu = 1486.6$ eV, for the first, Ni monolayer on Pd(1 1 1), model as a function of the film thickness.

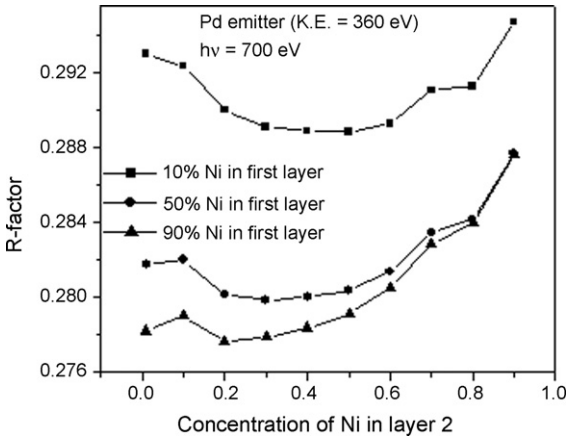

Fig. 5. *R*-factor analysis for the Pd 3d emitter in a Pd_xNi_{100-x} alloy emitting from two layers, indicating a minimum for the high Ni concentration in the first layer and low Ni concentration in the second layer.

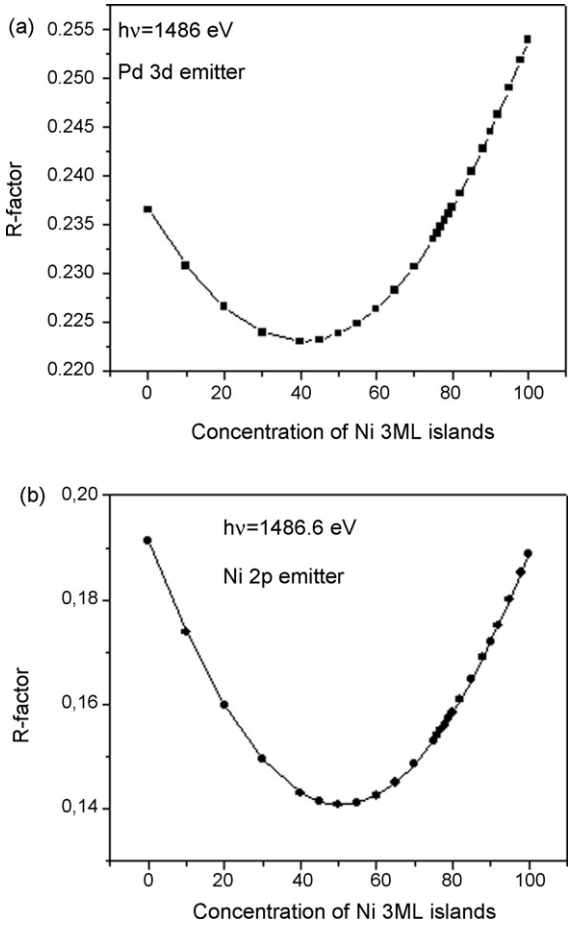

Fig. 6. *R*-factor analysis for the Ni and Pd emitter using a linear combination of a Ni_xPd_{100-x} alloy and a 3 ML Ni film ML as a function of the fraction of Pd(1 1 1) surface covered by Ni islands, indicating a minimum for the Ni island coverage of 50–60%.

consider the third model, where the surface is covered by Pd islands and by a $Pd_{20}Ni_{80}$ alloy extending several layers into the bulk, the R_a-factor decreases to 0.4. For the third model, we present, in Fig. 2, the corresponding experimental and theoretical Ni 3p and Pd 3d XPD curves excited with $h\nu = 700$ eV for the Pd film on Ni(1 1 1) annealed at 650 °C. In Fig. 2, we present the anisotropy, defined as $(I - I_0)/I_0$, where I is the experimental intensity and I_0 is an intensity averaged over all azimuthal angles and is different for each polar angle.

Our final conclusions [15] are that the Ni(1 1 1) surface is covered by regions of Pd bi-dimensional islands and by a $Pd_{20}Ni_{80}$ alloy, and that the Pd islands cover approximately 75% of the surface. A refinement in the structural parameters yields a distance between Pd atoms of 2.66 Å, which corresponds to a 3.3% compression compared to the Pd–Pd bulk value (2.75 Å). The lateral lattice parameter for the Pd_xNi_{100-x} alloy remains the same as the Ni(1 1 1) bulk value (2.54 Å) [15]. Similar results were previously reported for Pd on Cu(1 1 1) [17] and Cu on Pd(1 1 1) [20].

3.3. Ni on Pd(1 1 1) after annealing at 300 °C

Fig. 3 display Ni 2p and Pd 3d photoemission spectra excited by Al Kα radiation for a clean Pd (1 1 1) surface, after evaporation of approximately 3 ML of Ni on Pd(1 1 1) at room temperature, and after annealing at 300 and 600 °C. Annealing at 300 °C did not cause significant changes in the intensities of either Pd and Ni peaks with respect to the spectra of the deposited film. After annealing at 600 °C, however, the Ni signal almost disappeared, which indicates that Ni diffuses almost completely into the Pd bulk at this temperature. The LEED pattern for 3 ML of Ni evaporated on Pd(1 1 1) displayed a (1 × 1) pattern. Annealing at 300 °C for 30 min caused an enhancement of the (1 × 1) pattern, which is similar to that of Pd(1 1 1) [16].

In treating this problem, our procedure was analogous to that we used for Pd on Ni(1 1 1). We considered the following models: (1) fcc Ni overlayers on Pd(1 1 1), (2) a random Ni_xPd_{100-x} alloy, and (3) coexistence of regions with 0–4 ML thick Ni islands and alloy regions. For each model, the inter-layer and intra-layer distances were relaxed.

In Fig. 4, we present the final results of the monolayer model for the Pd 3d (Fig. 4(a)) and Ni 3p (Fig. 4(b)) and 2p (Fig. 4(c)) emitters. From Fig. 4(a), we observe that best result for the Pd emitter corresponds to the clean surface (i.e., 0 ML film thickness), which, in analogy to the case of Pd on Ni(1 1 1), indicates the existence of regions free of Ni overlayers: that is, a surface partially covered by Ni islands. From Fig. 4(b and c), we note that the best results for both Ni emitters correspond to island thicknesses of 3 ML, a result consistent with that from Fig. 4(a) since the Pd photoelectron's mean free path is too small to permit passage through a 3 ML film. We should note that the results for the island thickness should be considered as a sort of average: it is entirely possible that islands with different thicknesses from 1 to 4 ML coexist on the surface, a situation which we cannot treat at present. The first and second interplanar distances for the 3 ML Ni islands on Pd(1 1 1) in Fig. 4 were fully relaxed, and yielded 2.20 and 2.22 Å, respectively (the interlayer distances for Pd(1 1 1) and Ni(1 1 1) are 2.25 and 2.03 Å, respectively). It

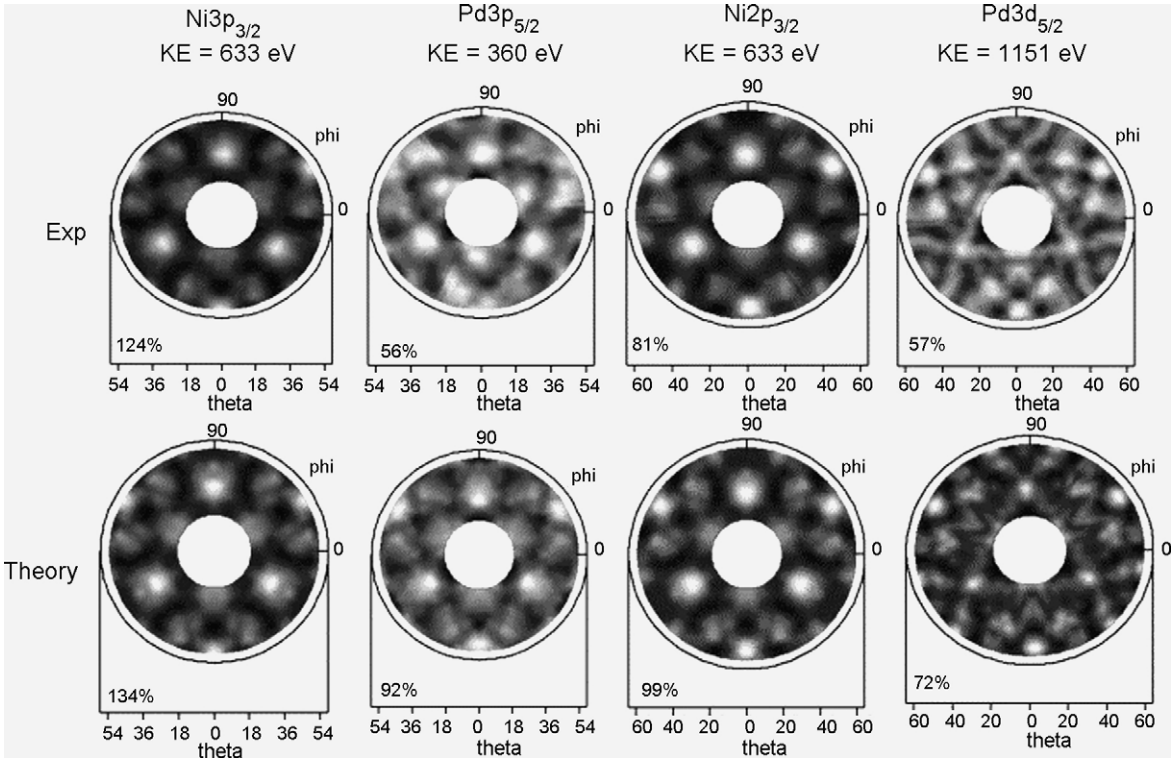

Fig. 7. Comparison of theory and experiment for Pd $3d_{5/2}$ and Ni $3p_{3/2}$ and $2p_{3/2}$ XPD patterns excited with $h\nu = 700$ eV and 1486.6 eV: (top) experimental patterns, (bottom) theoretical patterns (final results).

is clear that the interlayer distance decreases for Ni on Pd(1 1 1), which is consistent with the difference between the bulk Ni and bulk Pd lattice parameters (3.52 Å and 3.89 Å, respectively). The interplanar distance of ultra-thin Ni films grown epitaxially on a Pd(1 0 0) substrate also decrease below a critical thickness [12].

Again in analogy with the case of Pd on Ni(1 1 1), we analyzed the second model, a random Ni_xPd_{100-x} alloy: the results for the Pd 3d ($h\nu = 700$ eV) emitter is presented in Fig. 5. We tested different Ni concentrations in the first and second layers, and the best results indicate high Ni concentration, approximately 90%, in the first layer and low Ni concentration, around 20–40%, in the second layer. In particular, the *R*-factor from the Pd emitter for the random alloy model, ~0.27, is lower than that for a clean surface in Fig. 4(a), or 0.30, which suggests that the surface has island and random alloy regions. The first and second interplanar distances for the Ni_xPd_{100-x} alloy were also relaxed, and yielded 2.19 and 2.18 Å, respectively, so that both the first and second interlayer distances contract with respect to Pd(1 1 1). We believe that this contraction is an effect caused by the smaller size of Ni (the metallic radii of Ni and Pd are 1.25and 1.37 Å, respectively) [7].

In Fig. 6, we present our results for the statistical XPD analysis, which are similar to that described for Pd on Ni(1 1 1): the structural parameters and concentrations reported above were fixed and the percentage of the area covered by the islands was varied. We can infer from Fig. 6 that the 3 ML islands of nickel cover approximately 50–60% of the surface, and that the rest of the surface consists of alternating alloy layers having high (approximately 90%) and low (approximately 20–40%) concentrations of nickel. Fig. 7 presents the experimental (a) and final theoretical (b) XPD Ni $3p_{3/2}$, Ni $2p_{3/2}$ and Pd $3d_{5/2}$ XPD patterns. The Ni 3p and 2p data were taken with 700 and 1486.6 eV photon energies, respectively, and the Pd 3d spectra were obtained using both 700 and 1486.6 eV photon energies. The structural parameters and concentrations used in the theoretical calculations were those we discussed above and elsewhere [15,16].

4. Conclusions

Palladium and nickel ultra-thin films were deposited on Ni(1 1 1) and Pd(1 1 1), respectively, and were characterized by XPS, LEED, and XPD. Both Pd and Ni films grow in a layer-by-layer mode at room temperature.

For the 1.5 ML Pd film on Ni(1 1 1), LEED shows a reconstructed pattern at room temperature, which is attributed to a mosaic distribution of bi-dimensional Pd islands on the Ni(1 1 1) surface with a different lateral lattice parameter from that of Ni(1 1 1). Annealing the film at 650 °C brings back the (1 × 1) pattern, suggesting Pd diffusion and alloy formation. XPD analysis indicates that Pd diffuses at least to the 4th layer into the Ni(1 1 1) substrate in low concentration (10–20%), and that 75% of the surface remains covered with Pd bi-dimensional islands.

For the 3 ML Ni film on Pd(1 1 1), LEED exhibits a diffuse (1 × 1) pattern. After annealing at 600 °C, Ni diffuses completely into the Pd substrate. Annealing at 300 °C causes an enhancement of the (1 × 1) pattern. XPD analysis indicates that 3 ML Ni islands cover part of the surface (50–60%), and the other part is formed by a Ni_xPd_{100-x} alloy having alternating layers of high (approximately 90%) and low (approximately 20–40%) concentrations of nickel.

Acknowledgment

This work received financial support from FAPESP, CAPES, CNPq, and LNLS (SGM project #2195) of Brazil.

References

[1] J.A. Rodriguez, Surf. Sci. Rep. 24 (1996) 224.
[2] H. Dreyssé, C. Demangeat, Surf. Sci. Rep. 28 (1997) 65.
[3] G. Bozzolo, R.D. Noebe, J. Khalil, J. Morse, Appl. Surf. Sci. 219 (2003) 149.
[4] P. Miegge, J.L. Rousset, B. Tardy, J. Massardier, J.C. Bertolini, J. Catal. 149 (1994) 404.
[5] J.C. Bertolini, P. Miegge, P. Hermann, J.L. Rousset, B. Tardy, Surf. Sci. 331–333 (1995) 651.
[6] G.N. Derry, C.B. McVey, P.J. Rous, Surf. Sci. 326 (1995) 59.
[7] A. Christensen, A.V. Ruban, H.L. Skriver, Surf. Sci. 383 (1997) 235.
[8] A.C. Michel, L. Lianos, J.L. Rousset, P. Delichière, N.S. Prakash, J. Massardier, Y. Jugnet, J.C. Bertolini, Surf. Sci. 416 (1998) 288.
[9] S. Helfensteyn, J. Luyten, L. Feyaerts, C. Cremers, Appl. Surf. Sci. 212–213 (2003) 844.
[10] P. Hermann, B. Tardy, D. Simon, J.M. Guigner, B. Bigot, J.C. Bertolini, Surf. Sci. 307–309 (1994) 422.
[11] S. Terada, T. Yokoyama, N. Saito, Y. Okamoto, T. Ohta, Surf. Sci. 433–435 (1999) 657.
[12] G.A. Rizzi, M. Petukhov, M. Sambi, G. Granozzi, Surf. Sci. 522 (2003) 1.
[13] G.A. Rizzi, A. Cossaro, M. Petukhov, F. Sedona, G. Granozzi, F. Bruno, D. Cvetko, A. Morgante, L. Floreano, Phys. Rev. B 70 (2004) 045412.
[14] Y. Manzhur, P.M. Imielski, K. Potzger, W.D. Brewer, M. Dietrich, M.J. Prandolini, H.H. Bertschat, Eur. Phys. J. B 46 (2005) 535.
[15] M.F. Carazzolle, S.S. Maluf, A. de Siervo, P.A.P. Nascente, R. Landers, G.G. Kleiman, Surf. Sci. 600 (2006) 2268.
[16] M.F. Carazzolle, S.S. Maluf, A. de Siervo, P.A.P. Nascente, R. Landers, G.G. Kleiman, J. Electron Spectrosc. Rel. Phenom. 156–158 (2006) 405.
[17] A. de Siervo, E.A. Soares, R. Landers, T.A. Fazan, J. Morais, G.G. Kleiman, Surf. Sci. 504 (2002) 215.
[18] Y. Chen, M.A. Van Hove, MSCD-Multiple Scattering Calculation Diffraction Package. Available from: <http://www.sitp.lbl.gov>.
[19] E.A. Soares, A. de Siervo, R. Landers, G.G. Kleiman, Surf. Sci. 497 (2002) 205.
[20] A. de Siervo, R. Paniago, E.A. Soares, H.-D. Pfannes, R. Landers, G.G. Kleiman, Surf. Sci. 575 (2005) 217.